

# Relationship between resistivity, diffusivity and microstructural descriptors for mortars with silica fume

Peter J. Tumidajski\*

*St. Lawrence Cement, 3300 Highway 7, Suite 600, Concord, Ontario, Canada L4K 4M3*

Received 12 May 2004; accepted 1 October 2004

## Abstract

Mortars with a sand-to-cement ratio of 3 and water-to-cement ratio of 0.5 were made with 0% and 10% silica fume (SF). Resistivities were measured with alternating current impedance spectroscopy (ACIS). Diffusivities were determined with the propan-2-ol counterdiffusion method. Microstructure was investigated with mercury intrusion porosimetry. It was found that there is a relationship relating hydration time to the product of resistivity and diffusivity. Furthermore, the product of resistivity and diffusivity was related to porosity, mean and threshold pore diameters. The influence of silica fume in refining the pore structure was marked.

© 2004 Elsevier Ltd. All rights reserved.

**Keywords:** Pore size distribution; Diffusion; Electrical properties; Silica fume

## 1. Introduction

The durability of cementitious systems depends, to a great degree, on the diffusion and subsequent reaction of ionic species. Diffusivities are determined, in general, using difficult and time-consuming measurements. In an earlier paper [1], the formation factor ( $F$ ) was examined in an attempt to simply and rapidly determine diffusivities via Eq. (1).

$$F = \frac{\rho_{\text{mortar}}}{\rho_{\text{porewater}}} = \frac{D_{\text{porewater}}}{D_{\text{mortar}}} \quad (1)$$

where  $\rho$  and  $D$  represent resistivity and diffusivity, respectively. The difficulty with Eq. (1) lies with the choice of values for  $\rho_{\text{porewater}}$  and  $D_{\text{porewater}}$ .

In another study [2],  $F$  was related to the porosity ( $\varepsilon$ ) microstructural descriptor, with the Archie's Law relationship.

$$F = \mu \varepsilon^m \quad (2)$$

where  $m$  is a constant, and  $\mu$  is defined as  $\tau^2/\kappa$ , wherein  $\tau$  is tortuosity and  $\kappa$  is constrictivity. There was good agreement with Archie's law.

It is the purpose of the present study to extend the previous investigations in several ways. The first purpose is to determine if there exists a direct relationship between  $D_{\text{mortar}}$  and  $\rho_{\text{mortar}}$  without the complication of determining or assuming values for  $\rho_{\text{porewater}}$  and  $D_{\text{porewater}}$ . The second purpose is to determine if there is a relationship between the threshold and mean pore diameters ( $\delta_{\text{threshold}}$  and  $\delta_{\text{mean}}$ ) and the transport properties ( $D_{\text{mortar}}$  and  $\rho_{\text{mortar}}$ ). Finally, the development of mortar microstructure as silica fume (SF) replaces Portland cement is reported with data from mercury intrusion porosimetry.

## 2. Experimental

### 2.1. Materials

The cementitious materials were Type I Portland cement and silica fume (SF). The former had an aluminates ( $C_3A$ ) content of 11.82%. The SF had the following composition:  $SiO_2=95.2\%$ , carbon=1.56%,

\* Tel.: +1 905 761 7100x203; fax: +1 905 761 7200.

E-mail address: [Peter.Tumidajski@Holcim.com](mailto:Peter.Tumidajski@Holcim.com).

Table 1  
Experimental results

Time [days]	Resistivity ( $\rho$ ) [ $\Omega$ cm]	Diffusivity ( $D$ ) [ $\text{cm}^2 \text{s}^{-1}$ ]	Porosity ( $\varepsilon$ )	Threshold pore diameter ( $\delta_{\text{threshold}}$ ) [ $\mu\text{m}$ ]	Mean pore diameter ( $\delta_{\text{mean}}$ ) [ $\mu\text{m}$ ]
<i>w/c=0.5, s/c=3.0, SF=0%</i>					
1	$0.78 \times 10^4$	$1.52 \times 10^{-6}$	0.230	0.042	0.145
3	$1.19 \times 10^4$	$1.49 \times 10^{-6}$	0.227	0.030	0.126
7	$1.96 \times 10^4$	$1.46 \times 10^{-6}$	0.201	0.029	0.072
28	$5.47 \times 10^4$	$1.08 \times 10^{-6}$	0.189	0.023	0.041
<i>w/c=0.5, s/c=3.0, SF=10%</i>					
1	$0.17 \times 10^4$	$3.14 \times 10^{-6}$	0.253	0.087	0.083
3	$0.95 \times 10^4$	$1.77 \times 10^{-6}$	0.238	0.025	0.033
7	$5.58 \times 10^4$	$0.58 \times 10^{-6}$	0.208	0.018	0.023
28	$13.3 \times 10^4$	$0.52 \times 10^{-6}$	0.183	0.012	0.016

$\text{K}_2\text{O}=0.27\%$ ,  $\text{Na}_2\text{O}=0.10\%$ , with a surface area of 21,000  $\text{m}^2/\text{kg}$ . The sand for the mortar was Ottawa silica sand (ASTM C109).

## 2.2. Specimens

The sand-to-cementitious binder ratio (s/c) for the mortar specimens was three. The water-to-cementitious binder ratio was 0.5. The cementitious binders were prepared with 0% or 10% replacement of the Portland cement with SF. All mortars were hydrated at 100% relative humidity for 1, 3, 7 and 28 days.

The procedure for preparing the mortar was as follows. Cement was mixed with a portion of the water in a Hobart Model N-50 mixer (ASTM C305). The remaining water was then added while mixing at a slow speed for 2 min. SF was added and mixed at a low speed for 2 min and at a medium speed for another 2 min. Finally, the sand was added and mixed at slow speed for 2 min and at medium speed for 3 min. For the resistivity measurements, the mortar was cast into Plexiglass cubes ( $2.54 \times 2.54 \times 2.54$  cm) with stainless-steel electrodes on two opposite faces. For the diffusivity and porosimetry measurements, the mortar was cast into cylinders (3 cm o.d.  $\times$  15 cm).

## 2.3. Procedure

Mortar resistivities were determined with an alternating current impedance spectroscopy (ACIS) technique described by Gu et al. [3]. Impedance data were collected using an impedance gain-phase analyzer (Schlumberger Technologies Model 1260). Measurements were made logarithmically down in frequency range from 20 MHz to 1 Hz with 10 readings per decade.

Diffusivities were determined using the propan-2-ol counterdiffusion technique described in detail by Feldman [4]. Mortar discs approximately 1.14 mm thick (25 g) were cut from the cast cylinder, wiped free of excess

water and weighed. Subsequently, the discs were immersed in a very large volume (1.5 l) of anhydrous propan-2-ol. The weight of the discs was recorded every few minutes, and the propan-2-ol was renewed after 1, 2, 4, 8 and 24 h, and then every 24 h and less frequently after 7 days. The water-saturated mortar disc loses weight when immersed in propan-2-ol because the dense water is replaced by lighter propan-2-ol. Values of the propan-2-ol diffusivity are calculated from Fick's law in the form,

$$\frac{W_t}{W_\infty} = 1.127 \sqrt{\frac{D_m t}{L^2}} \quad (3)$$

where  $D_m$  is the propan-2-ol diffusivity into the mortar,  $t$  is the time,  $L$  is the half thickness of the specimen,  $W_t$  is the quantity of propan-2-ol diffusing through the pores into the specimen, and  $W_\infty$  is the quantity of

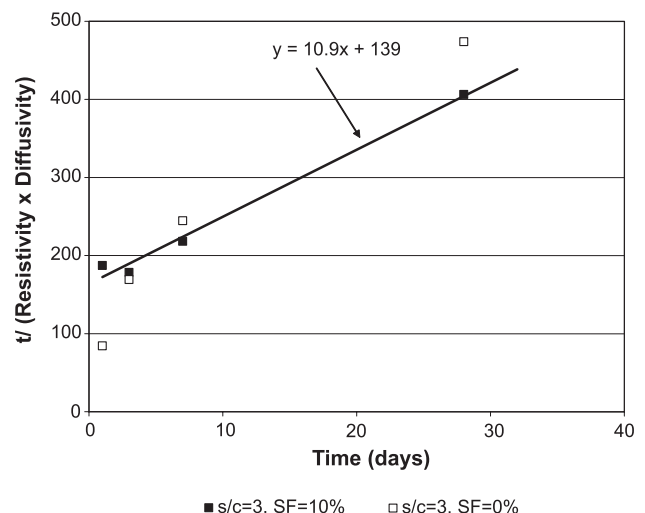


Fig. 1. Plot of  $t/(D_{\text{mortar}}\rho_{\text{mortar}})$  vs.  $t$ .

propan-2-ol at equilibrium (at approximately 2 weeks of immersion).

To determine the pore structure parameters at 1, 3, 7 and 28 days, hydration was arrested by immersion of mortar portions in propan-2-ol and then vacuum dehydrated at 105 °C. Subsequently, an Aminco-Winslow porosimeter was used to determine the pore size distribution and porosity of the samples. The instrument is capable of measurements in the range 0.005–45  $\mu\text{m}$ . Three individual mortar samples, designated Series 1 to 3, were run for each hydration condition.

### 3. Results

The experimental results for resistivity and diffusivity have been summarized in Table 1. It can be seen, for both mortars, that the resistivities increase and diffusivities decrease as hydration times increase, as expected. Comparing mortars with and without SF additions, the results show that the addition of SF results in higher resistivities, but only after 7 days of hydration. At hydration times earlier than 7 days, the addition of SF actually results in lower resistivities compared with

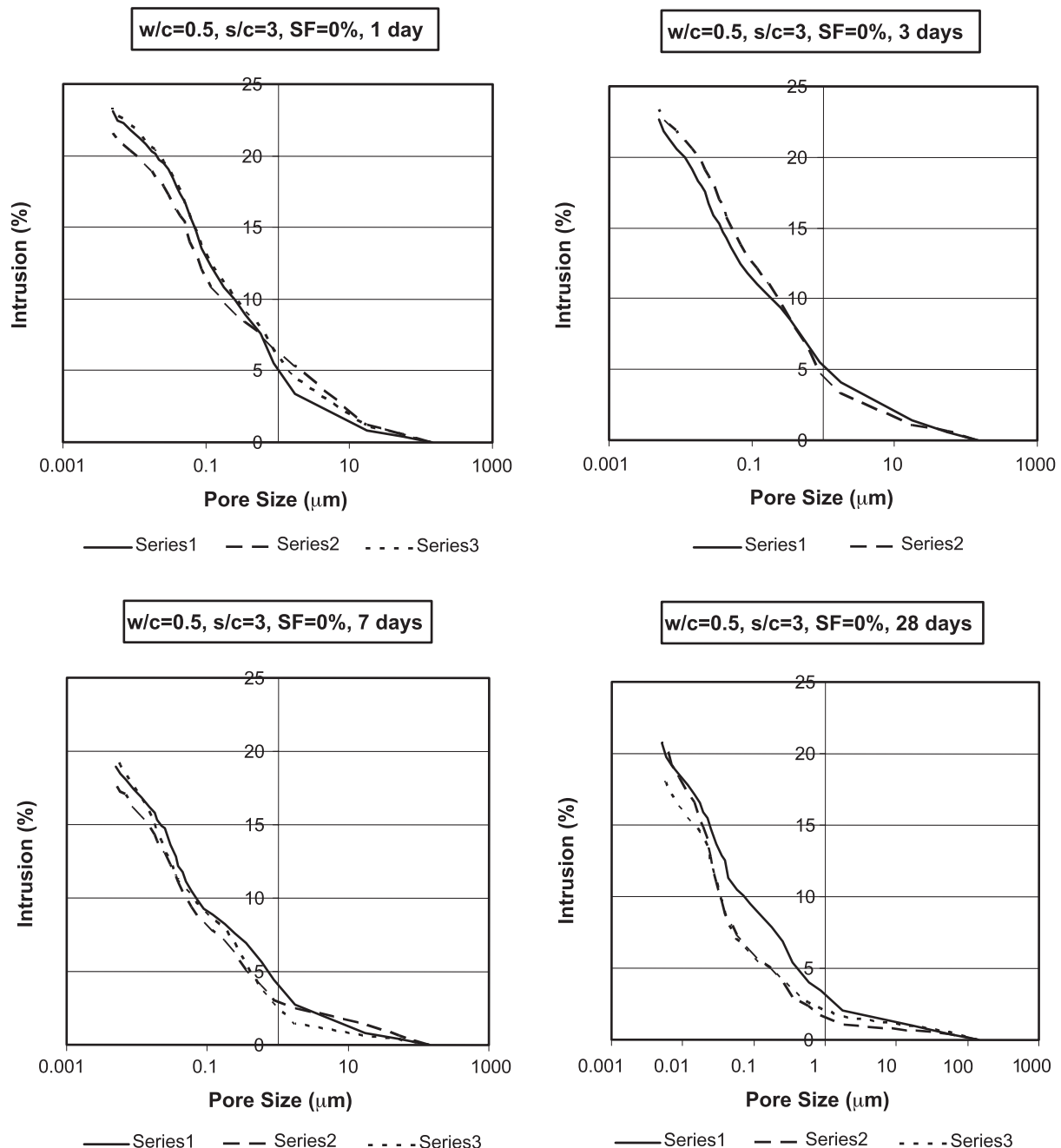


Fig. 2. Mercury intrusion porosimetry for mortars without silica fume.

mortars without SF addition. Results for diffusivity agree with the resistivity results. At early hydration times, the addition of SF results in larger values for the diffusivity, and it is only after 7 days of hydration that the diffusivities for mortars with SF are lower than that of mortars without SF. As hydration time increases, the products of resistivity and diffusivity appear to asymptotically approach a limit in a hyperbolic fashion. Accordingly, Fig. 1 is a plot of  $t/(\rho D)$  versus  $t$ . It can be seen that a linear relationship is indicated for the experimental

data with 0% and 10% SF. The relationships between  $(\rho D)$  and  $t$  is,

$$(\rho D) = \frac{t}{10.9t + 139} \quad (4)$$

The correlation coefficient for the fit to the experimental data is 0.96. The functional form of Eq. (4) means that diffusivities can be determined at any time if the easily measured resistivities are available, and without the uncertain estimates of  $\rho_{\text{porewater}}$  and  $D_{\text{porewater}}$ .

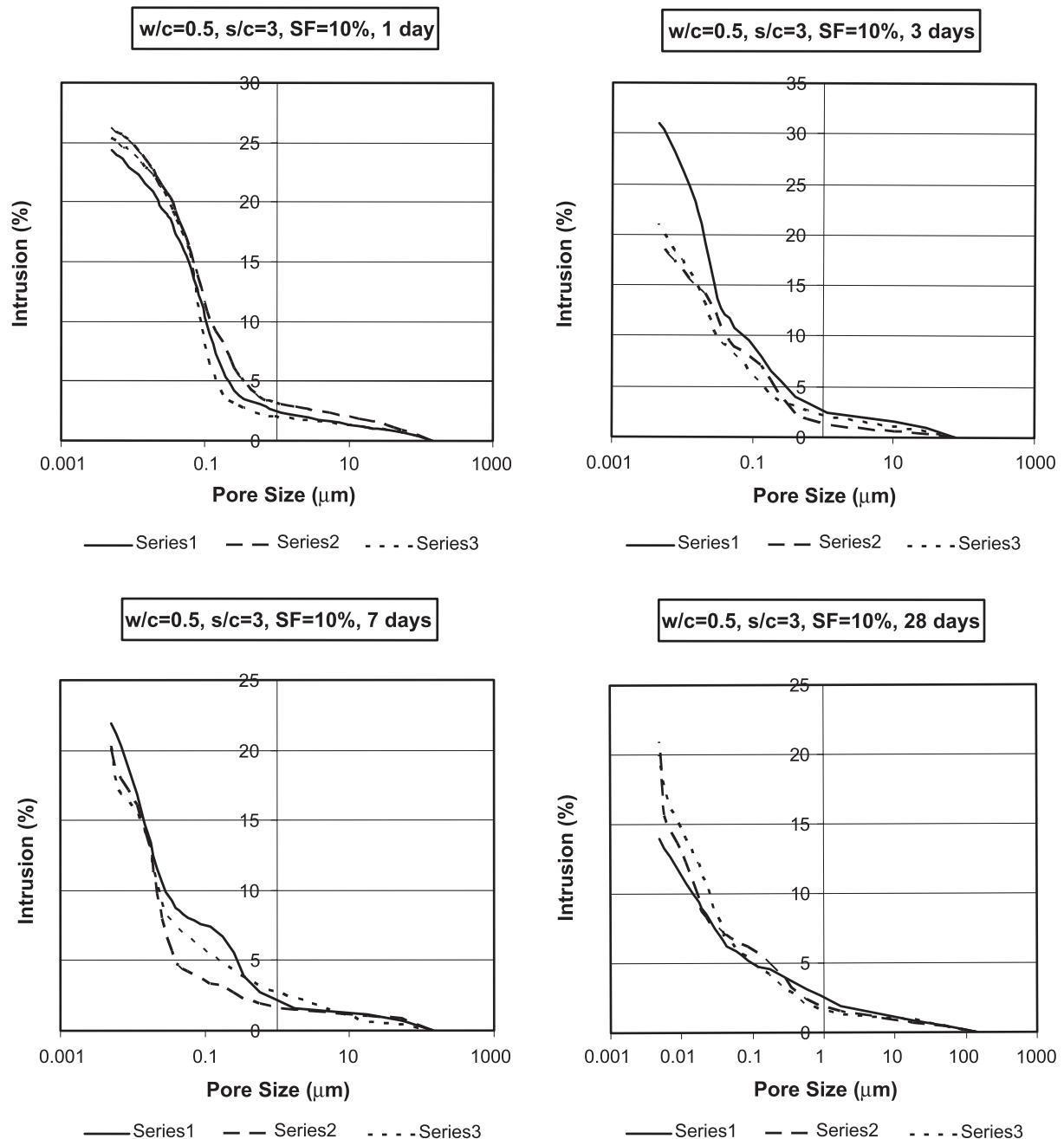


Fig. 3. Mercury intrusion porosimetry for mortars with silica fume.

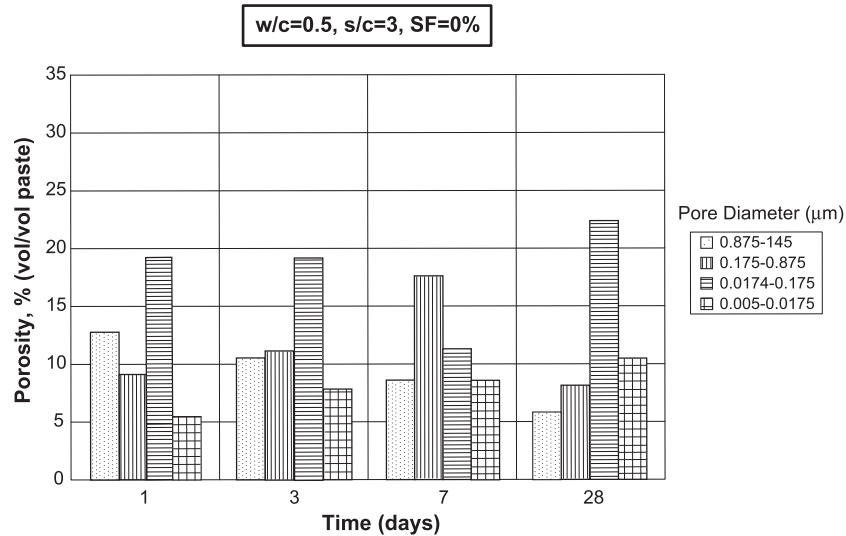


Fig. 4. Porosity histogram for mortars without silica fume.

Figs. 2 and 3 are the pore size distribution curves for mortars with 0% and 10% SF addition, respectively, at hydration times of 1, 3, 7 and 28 days. It can be seen that, for similar pore sizes, the pore volume of the samples without SF is higher than those with SF. For a curing time of 28 days and at a pore size  $0.1 \mu\text{m}$ , the pore volumes for mortars without SF and with SF are approximately 7.5% and 5%, respectively. Such behavior has been explained as due to a more discontinuous pore structure caused by reactions between SF and lime, especially around the sand grains [5]. Figs. 4 and 5 are histograms of the pore-size distribution, where the pore volume is based on the volume of the paste portion of the specimen. The histograms confirm the marked influence that SF additions have in skewing pore size distribution to the finer sizes compared with mortars without SF.

The porosity,  $\varepsilon$ , threshold pore diameter,  $\delta_{\text{threshold}}$ , and mean pore diameter,  $\delta_{\text{mean}}$ , determined from Figs. 2 and 3 are given in Table 1. Fig. 6 is a plot of  $\ln(\rho D)$  versus  $\ln(\varepsilon)$ . With a 0.96 correlation coefficient, the least-squares line is represented by,

$$\left(\frac{1}{\rho D}\right) = 2.1 \times 10^6 (\varepsilon)^{7.00} \quad (5)$$

The functional form of Eq. (5) follows from Archie's Law (Eq. (2)). In Eq. (5),  $m=7$ , which is larger than expected based on previous work on cement pastes and mortars, where  $m$  generally varies from 2 to 5 [2].

Fig. 7 is the plot of  $\ln(\rho D)$  versus  $\ln(\delta_{\text{threshold}})$ . It can be seen that the relationship between the two variables can be represented by the indicated least-squares line. Data for both 0% and 10% SF fall within the errors of the

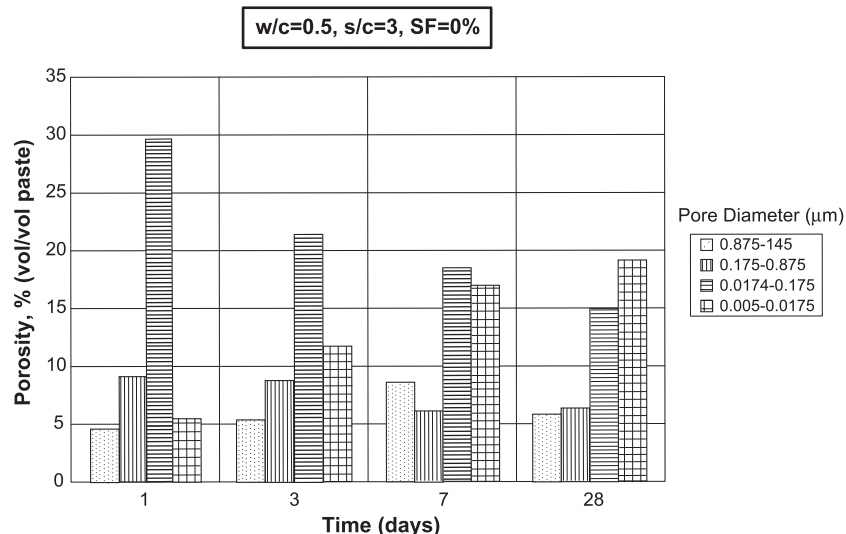
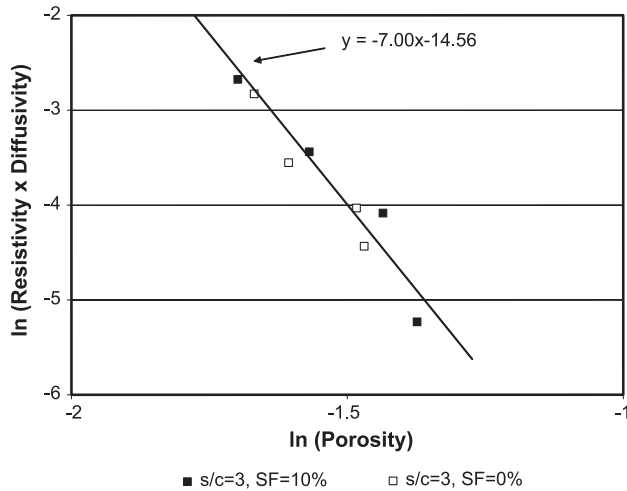


Fig. 5. Porosity histograms for mortars with silica fume.

Fig. 6. Plot of  $\ln(D_{\text{mortar}}\rho_{\text{mortar}})$  vs. porosity.

regression; however, the data points for the 0% SF at the lower values of  $\delta_{\text{threshold}}$  trend off the line. That said, the indicated regression has a correlation coefficient of 0.91 and is given by,

$$\left(\frac{1}{\rho D}\right) = 4.3 \times 10^3 (\delta_{\text{threshold}})^{1.28} \quad (6)$$

Despite the uncertainties in determining  $\delta_{\text{threshold}}$  from mercury intrusion experiments, percolation concepts have been used to relate the transport properties of porous media to microstructural descriptors. In the Katz-Thompson formula relating permeability and microstructural descriptors for rocks, the exponent for the critical pore diameter (which is equivalent to  $\delta_{\text{threshold}}$ ) has been theoretically determined to be 2 [6]. In this case, the exponent for  $\delta_{\text{threshold}}$  is seen to be 1.28. Eq. (6) represents an extension of previous work in that diffusivity was used and the microstructural descriptor was simplified to include only  $\delta_{\text{threshold}}$  [7].

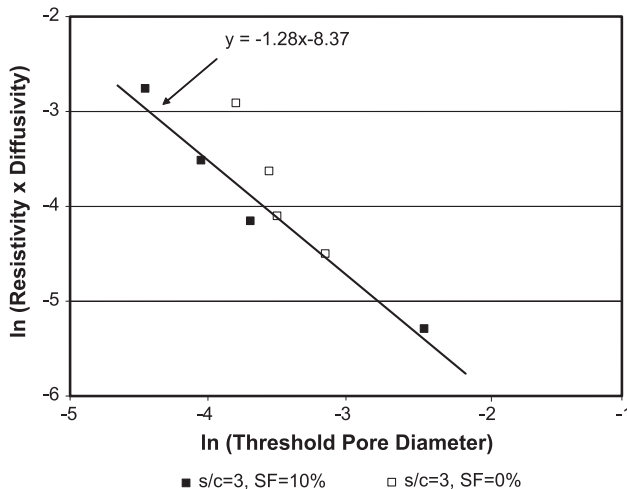
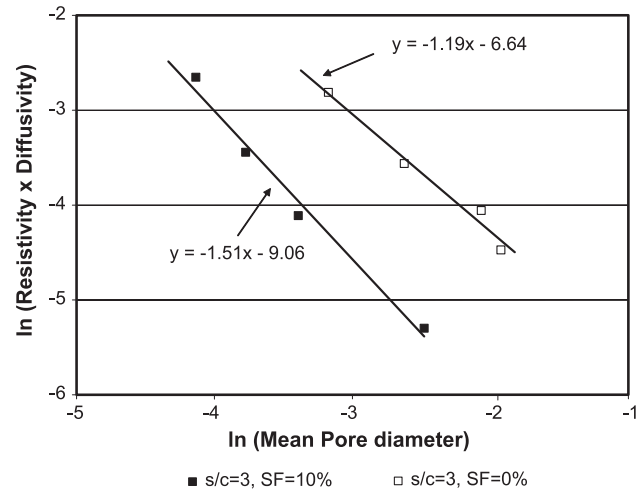
Fig. 7. Plot of  $\ln(D_{\text{mortar}}\rho_{\text{mortar}})$  vs. threshold pore diameter.Fig. 8. Plot of  $\ln(D_{\text{mortar}}\rho_{\text{mortar}})$  vs. mean pore diameter.

Fig. 8 is the plot of  $\ln(\rho D)$  versus  $\ln(\delta_{\text{mean}})$ . In contrast to Figs. 6 and 7, there are distinct relationships for the 0% and 10% SF mortars. The relationships are approximately parallel to each other, and, in both cases, the correlation coefficients for the linear fit are greater than 0.97. The relationships are given as,

$$\left(\frac{1}{\rho D}\right)_{0\% \text{SF}} = 764 (\delta_{\text{mean}})^{1.19} \quad (7a)$$

and,

$$\left(\frac{1}{\rho D}\right)_{10\% \text{SF}} = 8609 (\delta_{\text{mean}})^{1.51} \quad (7b)$$

for the mortars with 0% and 10% SF, respectively. It appears that  $\delta_{\text{mean}}$  microstructural descriptor is better able to discriminate the influence of SF additions on the resulting durability ( $\rho D$ ) parameter.

The excellent correlation coefficients ( $R > 0.90$ ), as represented in Figs. 6–8, between ( $\rho D$ ) and the microstructural descriptors, as determined from mercury intrusion porosimetry, indicate that the porosity that is accessible to mercury accounts for the bulk of the isopropanol exchange.

#### 4. Conclusions

1. There is a relationship between the durability parameter ( $D_{\text{mortar}}\rho_{\text{mortar}}$ ) and hydration time. Values for  $\rho_{\text{porewater}}$  and  $D_{\text{porewater}}$  are not required.
2. There are linear relationships between ( $D_{\text{mortar}}\rho_{\text{mortar}}$ ) and the microstructural descriptors obtained from mercury intrusion porosimetry ( $\epsilon$ ,  $\delta_{\text{threshold}}$  and  $\delta_{\text{mean}}$ ).
3. Diffusivities are time consuming to determine directly by experiment. By using electrochemical measurements in conjunction with mercury intrusion porosimetry, it is possible to quickly and simply calculate diffusivities.

## References

- [1] P.J. Tumidajski, A.S. Schumacher, On the relationship between formation factor and diffusivity in mortars, *Cem. Concr. Res.* 26 (8) (1996) 1301–1306.
- [2] P.J. Tumidajski, A.S. Schumacher, S. Perron, P. Gu, J. Beaudoin, On the relationship between porosity and electrical resistivity in cementitious systems, *Cem. Concr. Res.* 26 (4) (1996) 539–544.
- [3] P. Gu, P. Xie, J. Beaudoin, R. Brousseau, A.C. impedance spectroscopy: I. A new equivalent circuit model for hydrated cement paste, *Cem. Concr. Res.* 22 (1992) 833–840.
- [4] R.F. Feldman, Diffusion measurements in cement paste by water replacement using propan-2-ol, *Cem. Concr. Res.* 17 (1987) 602–612.
- [5] H. Cheng, R.F. Feldman, Influence of silica fume on the microstructural development in cement mortars, *Cem. Concr. Res.* 15 (2) (1985) 285–294.
- [6] A.J. Katz, A.H. Thompson, Quantitative prediction of permeability in porous rocks, *Phys. Rev., B* 34 (1986) 8179–8181.
- [7] P.J. Tumidajski, B. Lin, On the validity of the Katz-Thompson Equation for permeabilities in concrete, *Cem. Concr. Res.* 28 (5) (1998) 643–647.